Journal of Hazardous Materials 190 (2011) 574–581

Contents lists available at ScienceDirect

Journal of Hazardous Materials

journal homepage: www.elsevier.com/locate/jhazmat

The interaction between 4-aminoantipyrine and bovine serum albumin: Multiple spectroscopic and molecular docking investigations

Yue Teng[a], Rutao Liu[a,*], Chao Li[b], Qing Xia[a], Pengjun Zhang[a]

[a] Shandong Key Laboratory of Water Pollution Control and Resource Reuse, School of Environmental Science and Engineering, Shandong University, China-America CRC for Environment & Health, Shandong Province, 27# Shanda South Road, Jinan 250100, PR China
[b] Shandong University Hospital, 91# Shanda North Road, Jinan 250100, PR China

ARTICLE INFO

Article history:
Received 26 January 2011
Received in revised form 22 March 2011
Accepted 22 March 2011
Available online 29 March 2011

Keywords:
4-Aminoantipyrine
Bovine serum albumin
Multi-spectroscopic techniques
Toxicity evaluation

ABSTRACT

4-Aminoantipyrine (AAP) is widely used in the pharmaceutical industry, in biochemical experiments and in environmental monitoring. AAP as an aromatic pollutant in the environment poses a great threat to human health. To evaluate the toxicity of AAP at the protein level, the effects of AAP on bovine serum albumin (BSA) were investigated by multiple spectroscopic techniques and molecular modeling. After the inner filter effect was eliminated, the experimental results showed that AAP effectively quenched the intrinsic fluorescence of BSA via static quenching. The number of binding sites, the binding constant, the thermodynamic parameters and binding subdomain were measured, and indicated that AAP could spontaneously bind with BSA on subdomain IIIA through electrostatic forces. Molecular docking results revealed that AAP interacted with the Glu 488 and Glu 502 residues of BSA. Furthermore, the conformation of BSA was demonstrably changed in the presence of AAP. The skeletal structure of BSA loosened, exposing internal hydrophobic aromatic ring amino acids and peptide strands to the solution.

1. Introduction

Serum albumins are the major soluble proteins of the circulatory system (accounting for 50–60% of the total plasma protein) [1]. Serum albumins have many physiological functions [2]. The most important property of the abundant serum protein is that they serve as a transport vehicle for a variety of endogenous and exogenous compounds [3]. It has been shown that the distribution, free concentration and the metabolism of many biologically active compounds, such as metabolites, drugs and even some toxins, are correlated with their binding to serum albumin [4]. Furthermore, it has also been demonstrated that conformational changes of serum albumin can be caused by interactions with small molecule ligands, which may influence serum albumin's biological function as a carrier protein [5,6]. The interactions of serum albumin with ligands have attracted a great deal of interest for many years due to their application in a great variety of biological [7], pharmaceutical [8], toxicological [9] and cosmetic [10] systems. As the sequences of human serum albumin (HSA) and BSA are 76% similar, BSA is commonly substituted for HSA in experiments due to its availability and lower cost [11,12].

4-Aminoantipyrine (AAP, structure in the inset of Fig. 1) is a metabolite of aminophenazone and is an aromatic substance with analgesic, antipyretic and anti-inflammatory properties [13]. However, AAP usually produces side effects such as the risk of agranulocytosis [14]. Although AAP is scarcely ever administered as an analgesic because of side effects, as a raw material, it is mostly used to produce 4-aminoantipyrine derivatives, which have better biological activities [15,16]. In addition, it is used as a reagent for biochemical reactions producing peroxides or phenols [17,18] and can also be used to detect phenols in the environment [19]. Since AAP is widely used in the pharmaceutical industry, biochemical research and environmental monitoring, AAP has become an environmental pollutant.

The toxic effect of 4-aminoantipyrine on experimental animals has been reported [20]. AAP can reduce blood flow [21] and 13,14-dihydro-15-keto prostaglandin F2 alpha concentration [22] after it is infused into the blood. AAP can form stable complexes with heme [23]. The interaction of AAP with bovine hemoglobin has been studied in our laboratory and AAP has an obvious denaturing effect on bovine hemoglobin [24]. Considering the important physiological functions of serum albumin in circulatory system, it would be interesting to observe the effect of AAP on serum albumin. In the present work, we investigated the toxic effects of AAP on BSA under simulative physiological conditions by spectroscopic and molecular modeling methods. After considering the inner filter effect, we estimated the association constants, number of binding

* Corresponding author. Tel.: +86 531 88364868; fax: +86 531 88364868.
E-mail address: rutaoliu@sdu.edu.cn (R. Liu).

0304-3894/$ – see front matter © 2011 Elsevier B.V. All rights reserved.
doi:10.1016/j.jhazmat.2011.03.084

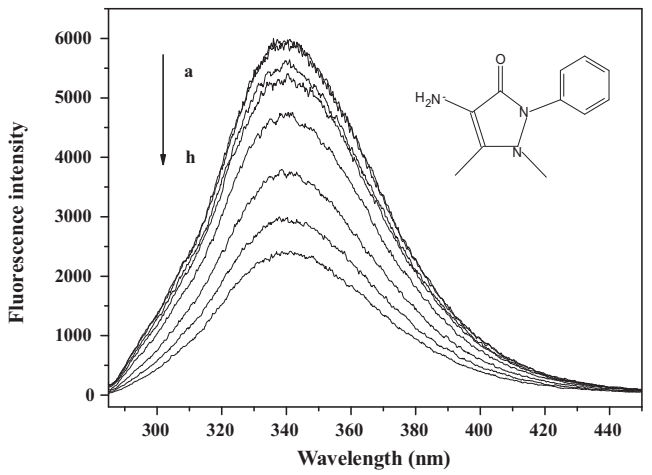

Fig. 1. The influence of AAP on the fluorescence emission spectra of BSA. *Conditions*: BSA – 1.0×10^{-6} mol L^{-1}; AAP – (a) 0 mol L^{-1}, (b) 1×10^{-6} mol L^{-1}, (c) 5×10^{-6} mol L^{-1}, (d) 1×10^{-5} mol L^{-1}, (e) 2×10^{-5} mol L^{-1}, (f) 4×10^{-5} mol L^{-1}, (g) 6×10^{-5} mol L^{-1}, (h) 8×10^{-5} mol L^{-1}; pH 7.4; T = 294 K.

sites, thermodynamic parameters, and binding force for the interaction of AAP with BSA. The specific binding site of AAP on BSA was investigated in detail. The effect of AAP on the microenvironment and conformation of BSA was also investigated. This study provides basic data for clarifying the binding mechanisms of AAP with serum albumin and is helpful for understanding its effect on protein function during its transportation in the blood and its toxicity in vivo.

2. Experimental

2.1. Reagents

Bovine serum albumin (BSA) was obtained from Sinopharm Chemical Reagent Co., Ltd. 4-Aminoantipyrine (AAP) was obtained from Tianjin Chemical Reagent Co. Ltd. AAP was dissolved with ultrapure water as a stock solution, 1.0×10^{-3} mol L^{-1}. Phenylbutazone (PB), flufenamic acid (FA), and digitoxin (Dig) were obtained from Tokyo Chemical Industry Co. Ltd. and were dissolved in ethanol to form a 1.0×10^{-3} mol L^{-1} solution, which was used to determine the binding sites of AAP on BSA. A 0.2 mol L^{-1} mixture of phosphate buffer (mixture of $NaH_2PO_4 \cdot 2H_2O$ and $Na_2HPO_4 \cdot 12H_2O$, pH 7.4) was used to control the pH. Ultrapure water (18.25 MΩ) was used throughout the experiments.

2.2. Apparatus and measurements

2.2.1. Fluorescence measurements

All fluorescence spectra were recorded on an F-4600 fluorescence spectrophotometer (Hitachi, Japan) with a 1 cm cell. The excitation wavelength was 278 nm. The excitation and emission slit widths were set at 5 nm. Scan speed was 1200 nm/min. PMT (Photo Multiplier Tube) voltage was 680 V.

Synchronous fluorescence spectra of BSA in the absence and presence of 4-aminoantipyrine were measured ($\Delta\lambda$ = 15 nm, λ_{ex} = 265–320 nm and $\Delta\lambda$ = 60 nm, λ_{ex} = 250–310 nm, respectively). The excitation and emission slit widths were set at 5 nm. Scan speed was 1200 nm/min. PMT voltage was fixed at 680 V.

2.2.2. UV–vis absorption measurements

The absorption spectra were recorded on a double beam UV-2450 spectrophotometer (Shimadzu, Japan) equipped with 1.0 cm quartz cells. Slit width was set at 2.0 nm. The wavelength range was 310–200 nm.

2.2.3. Circular dichroism (CD) measurements

CD spectra were made on a J-810 Spectropolarimeter (Jasco, Tokyo, Japan) in a 1-cm cell at room temperature. Bandwidth was 1 nm and scanning speed was 200 nm/min.

2.2.4. Molecule docking investigation

Docking calculations were carried out using AutoDock 4.2. The structure of AAP was generated by Materials Studio 4.4. With the aid of AutoDock, the ligand root of AAP was detected and rotatable bonds were defined.

As the crystal structure of BSA is unavailable in Protein Data Bank [25], a homologous model structure was used for the docking studies with AAP. A BLAST search in the PDB with a BSA sequence [Swissprot sequence ALBU_BOVIN (P02769)] revealed 75% identity with HSA. The SAM_T06 server was used to obtain the model structure, which has been used for previous docking studies [26–28]. AutoDock used the local search to search for the optimum binding site of small molecules to the protein. To recognize the binding sites in BSA, blind docking was carried out, with the grid size set to 110, 110 and 110 along the *X*-, *Y*- and *Z*-axes with 0.375 Å grid spacing. The center of the grid was set to 35.604, 4.724 and −24.211 Å. Maximum number of iterations was 300 and maximum number of successes/failures in a row before changing rho was 4. The conformation with the lowest binding free energy was used for further analysis.

3. Results and discussion

3.1. Fluorescence measurements

Fluorescence has been widely used to investigate the interaction between ligands and proteins and can give some information about the quenching mechanism, binding constants and binding sites.

The inner filter effect (IFE) would affect fluorescence measurements [29]. To determine whether an IFE induced by the absorption of excitation and emission radiation is significant in this system, we checked the sum of the absorbance at 278 nm (excitation wavelength) and 340.8 nm (fluorescence peak) under different conditions. The differences in the sums could cause no more than 5% percentage error for each sample, so IFE was ignored here.

Changes of emission spectra can provide information about their structure and dynamics [30]. Fluorescence emission spectra of BSA with different AAP concentrations were recorded at room temperature (Fig. 1). It can be seen from Fig. 1 that the fluorescence intensity decreased with the increasing concentration of AAP. The fluorescence quenching of BSA by AAP indicated that AAP can bind to BSA and alter the structure of BSA.

3.2. The fluorescence quenching mechanism

Since the intrinsic fluorescence of BSA can be quenched by AAP, we further explored the quenching mechanism. Quenching mechanisms are usually divided into dynamic quenching and static quenching. Since higher temperature results in larger diffusion coefficients, the dynamic quenching constants will increase with increasing temperature. In contrast, increased temperature is likely to result in decreased stability of complexes, and thus lower the value of the static quenching constants [31]. The quenching mode was primarily described as dynamic. In order to test this view, we used the well-known Stern–Volmer equation [32]:

$$\frac{F_0}{F} = 1 + K_{SV}[Q] = 1 + k_q \tau_0 [Q] \quad (1)$$

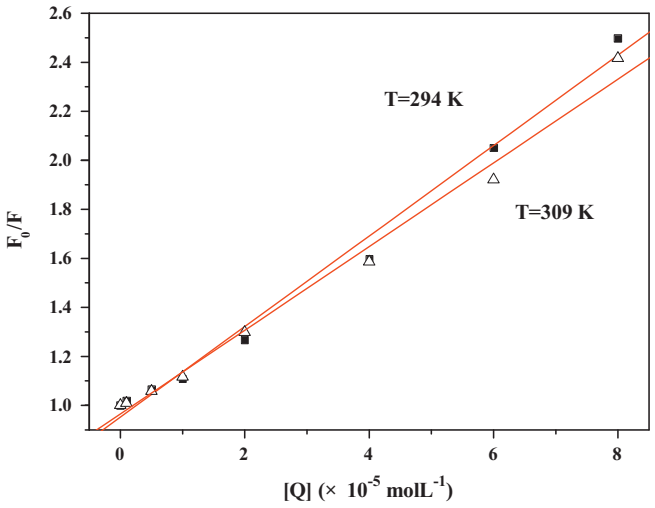

Fig. 2. Stern–Volmer plots for the quenching of BSA by AAP at 294 and 309 K.

Table 1
Stern–Volmer quenching constants for the interaction of AAP with BSA at 294 and 309 K.

T (K)	K_{SV} ($\times 10^4$ L mol^{-1})	k_q ($\times 10^{12}$ L mol^{-1} s^{-1})	R^a	S.D.[b]
294	1.85	1.85	0.9948	0.0611
309	1.71	1.71	0.9951	0.0552

[a] R is the correlation coefficient.
[b] S.D. is the standard deviation for the K_{SV} values.

where F_0 and F are the fluorescence intensity in the absence and presence of the quencher, [Q] is the concentration of the quencher, τ_0 is the fluorescence lifetime in the absence of quencher, and k_q is the quenching rate constant of the biological macromolecule. K_{SV} is the Stern–Volmer quenching constant.

Fluorescence intensity data were analyzed according to F_0/F versus [Q] at 294 and 309 K (Fig. 2.). Eq. (1) was applied to determine K_{SV} (Table 1) by a linear regression plot of F_0/F against [Q]. The value of k_q was also obtained (the fluorescence lifetime of the biopolymer (τ_0) is 10^{-8} s [33]).

The results showed that the K_{SV} values decreased with increasing temperature. Moreover, the maximum dynamic quenching constant k_q of the various quenchers is 2.0×10^{10} L mol^{-1} s^{-1} [34]. However, the values of k_q at 294 and 309 K are far greater than 2.0×10^{10} L mol^{-1} s^{-1}. Thus, the results indicated that the overall quenching is dominated by a static quenching mechanism forming an AAP–BSA complex.

3.3. Binding constant and binding capacity

For the static quenching interaction, when small molecules bind independently to a set of equivalent sites on a protein, the binding constant (K_a) and the number of binding sites (n) can be determined [35]. The relationship between the fluorescence intensity and the quenching medium can be deduced from the formula [36]:

$$lg\frac{(F_0 - F)}{F} = lg\ K_a + n\,lg[Q] \quad (2)$$

where F_0, F and [Q] are the same as in Eq. (1), K_a is the binding constant and n is the number of binding sites. The values of n and K_a (Table 2) were calculated and the number of binding sites n approximately equals 1, which can be concluded that there is one binding site in BSA for AAP during their interaction. The value of K_a is 8.19×10^4 L mol^{-1} in room temperature, indicating that a strong interaction exists between AAP and BSA. Even if a low concentration of AAP is present in the blood, AAP can interact with BSA easily.

3.4. Determination of the interaction forces between AAP and BSA

There are four types of interactions between small molecule ligands and biological macromolecules: hydrophobic forces, hydrogen bonds, van der Waals' interactions and electrostatic forces. The noncovalent interaction forces between proteins and small molecules can be determined by thermodynamic parameters. Ross and Subramanian [37] have summed up the thermodynamic laws to determine the types of binding with various interactions. If $\Delta H^\circ < 0$, $\Delta S^\circ < 0$, van der Waals and hydrogen bond interactions play the main roles in the binding reaction. If $\Delta H^\circ > 0$, $\Delta S^\circ > 0$, hydrophobic interactions are dominant. If $\Delta H^\circ < 0$, $\Delta S^\circ > 0$, the main force is an electrostatic effect.

$$\ln\left(\frac{K_2}{K_1}\right) = \left(\frac{1}{T_1} - \frac{1}{T_2}\right)\left(\frac{\Delta H^\circ}{R}\right) \quad (3)$$

$$\Delta G^\circ = -RT\ \ln K \quad (4)$$

$$\Delta G^\circ = \Delta H^\circ - T\Delta S^\circ \quad (5)$$

where K_1 and K_2 are the binding constants (analogous to K_a in Eq. (2)) at T_1 and T_2, and R is the universal gas constant.

When the change of temperature is small, ΔH° can be considered a constant, and can be approximated from Eq. (3). The free-energy change (ΔG°) and the entropy change (ΔS°) of the binding reaction follow Eqs. (4) and (5), respectively [38].

The values of the thermodynamic parameters were $\Delta H^\circ = -9.22$ kJ mol^{-1}, $\Delta G^\circ = -22.0$ kJ mol^{-1} and $\Delta S^\circ = 43.5$ J mol^{-1} K^{-1} at ambient temperature (shown in Table 2). Negative ΔG° means that the interaction process was spontaneous and the negative ΔH° and positive ΔS° indicated that electrostatic forces play the major role during the interaction. Because the pH (7.4) we used in the experimental conditions is much greater than the isoelectric point of BSA (pH 4.7), BSA is negatively charged. However, AAP is easily positively charged [39]. Positively charged AAP can spontaneously interact with the negatively charged BSA through electrostatic forces, which is in accordance with the calculated results of thermodynamic parameters. In our previous work [24], AAP could spontaneously bind with bovine

Table 2
Binding constants K_a and relative thermodynamic parameters of the AAP–BSA system.

T (K)	K_a ($\times 10^4$ L mol^{-1})	n	R^a	ΔH° (kJ mol^{-1})	ΔS° (J mol^{-1} K^{-1})	ΔG° (kJ mol^{-1})
294	8.19	1.163	0.9965	−9.22	43.5	−22.0
308	6.82	1.148	0.9988		43.6	−22.7

[a] R is the correlation coefficient for the K_a values.

Table 3
Effects of site probe on the binding constant of AAP on BSA.

K (without the site probe) (10^4 L mol^{-1})	K (with PB) (10^4 L mol^{-1})	K (with FA) (10^4 L mol^{-1})	K (with Dig) (10^4 L mol^{-1})
8.19	9.97	0.902	9.50

Table 4
Distance between the residues (8 Å involved) and AAP.

AAP atom (atom ID)	Protein atom (atom type)	Distance (Å)
C 24	Cys 484 O	3.19
C 6	His 487 O	2.96
C 1	Glu 488 CA	3.58
C 1	Lys 489 CA	6.35
C 1	Thr 490 CA	6.90
C 6	Pro 491 CB	3.33
C 6	Val 492 N	6.37
C 5	Ser 493 O	6.24
C 5	Glu 494 O	7.76
C 5	Thr 497 CG2	3.90
C 24	Cys 500 CB	3.71
O 16	Thr 501 CG2	3.39
N 17	Glu 502 N	6.59
N 17	Ser 503 HN	6.90
N 17	Gln 227 O	6.51
C 15	Lys 228 CD	3.94
N 17	Phe 229 CE1	5.24

hemoglobin through van der Waals forces and hydrogen bonds with one binding site. It can be seen from the results that AAP can bind to BSA and bovine hemoglobin through different binding modes.

3.5. Identification of binding sites on BSA

Similar to HSA, the globular protein BSA consists of three structurally similar domains (I, II, and III), each containing two subdomains (A and B) [40]. The principal regions of the ligand binding sites of albumin are located in two hydrophobic pockets in subdomains IIA and IIIA, namely site I and site II [41]. Many ligands bind specifically to serum albumin, for example warfarin and phenylbutazone (PB) for site I (subdomain IIA), flufenamic acid (FA) and ibuprofen for site II (subdomain IIIA) and digitoxin (Dig) for site III [42]. An assay to determine binding sites of AAP to BSA was done by fluorescence displacement measurement using the following specific probes: PB (site I), FA (site II) and Dig (site III). The changes in displacement experiments to determine the specificity of the binding site of AAP to BSA are shown in Table 3. AAP was not significantly displaced by PB or by Dig. However, FA gave a significant displacement of AAP, suggesting that the AAP binding site on BSA is subdomain IIIA, namely site II. So positively charged AAP can bind with the negatively charged BSA on the subdomain IIIA through electrostatic forces.

To further define the binding site, a molecule docking investigation was carried out. We predicted the positively charged AAP would mainly bind with the negatively charged amino acid residues (Glu and Asp) of BSA in subdomain IIIA, so we investigated the negatively charged amino acid residues in subdomain IIIA (Fig. 3). There are eight glutamates and two aspartates in subdomain IIIA. The exact binding site of AAP on BSA is shown in Fig. 4(A). We docked AAP to the 3D structure of BSA using AutoDock 4.2. This docking revealed the most likely binding site in the protein. The detailed docking results are shown in Fig. 4(C), and the distances are listed in Table 4. AAP bound to BSA on subdomain IIIA, which was exactly consistent with the site-competitive displacement experiments. The amino acid residues lining this binding site were Cys 484, His 487, Glu 488, Lys 489, Thr 490, Pro 491, Val 492, Ser 493, Glu 494, Thr 497, Cys 500, Thr 501, Glu 502, Ser 503, Gln 227, Lys 228 and Phe 229. The essential driving force of AAP binding to this site was electrostatic interaction. As shown in Fig. 4(C), there were electrostatic interactions between Glu 502 and two polar hydrogen atoms at position 17. The electrostatic interactions also existed between Glu 488 and the hydrogen atoms linked C18. The docking results revealed there was no hydrogen bonding between AAP and BSA. Van der Waals interactions existed, but the

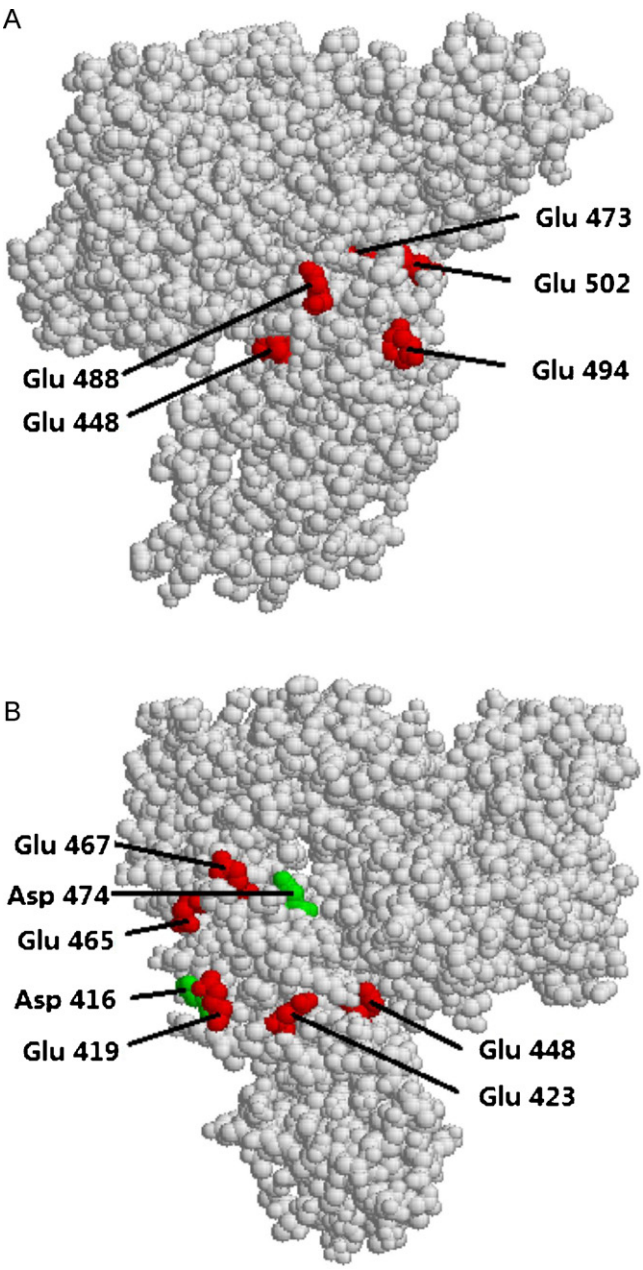

Fig. 3. (A and B) Negatively charged amino acid residues (Glu and Asp) of BSA in subdomain IIIA viewed from different perspectives.

electrostatic forces played a major role in the binding of AAP to BSA.

3.6. Conformational investigations

Since spectroscopy allows non-intrusive measurement of substances, it is a useful tool to investigate conformational changes of proteins, even at the low concentrations that are typical of physiological conditions [43]. To evaluate the effect of AAP on the conformation changes of BSA, synchronous fluorescence, UV–vis absorption and circular dichroism spectroscopy were used.

3.6.1. Synchronous fluorescence spectroscopy

Synchronous fluorescence spectroscopy can give information about the molecular environment in the vicinity of a chromophore such as tryptophan and tyrosine and it involves simultaneous

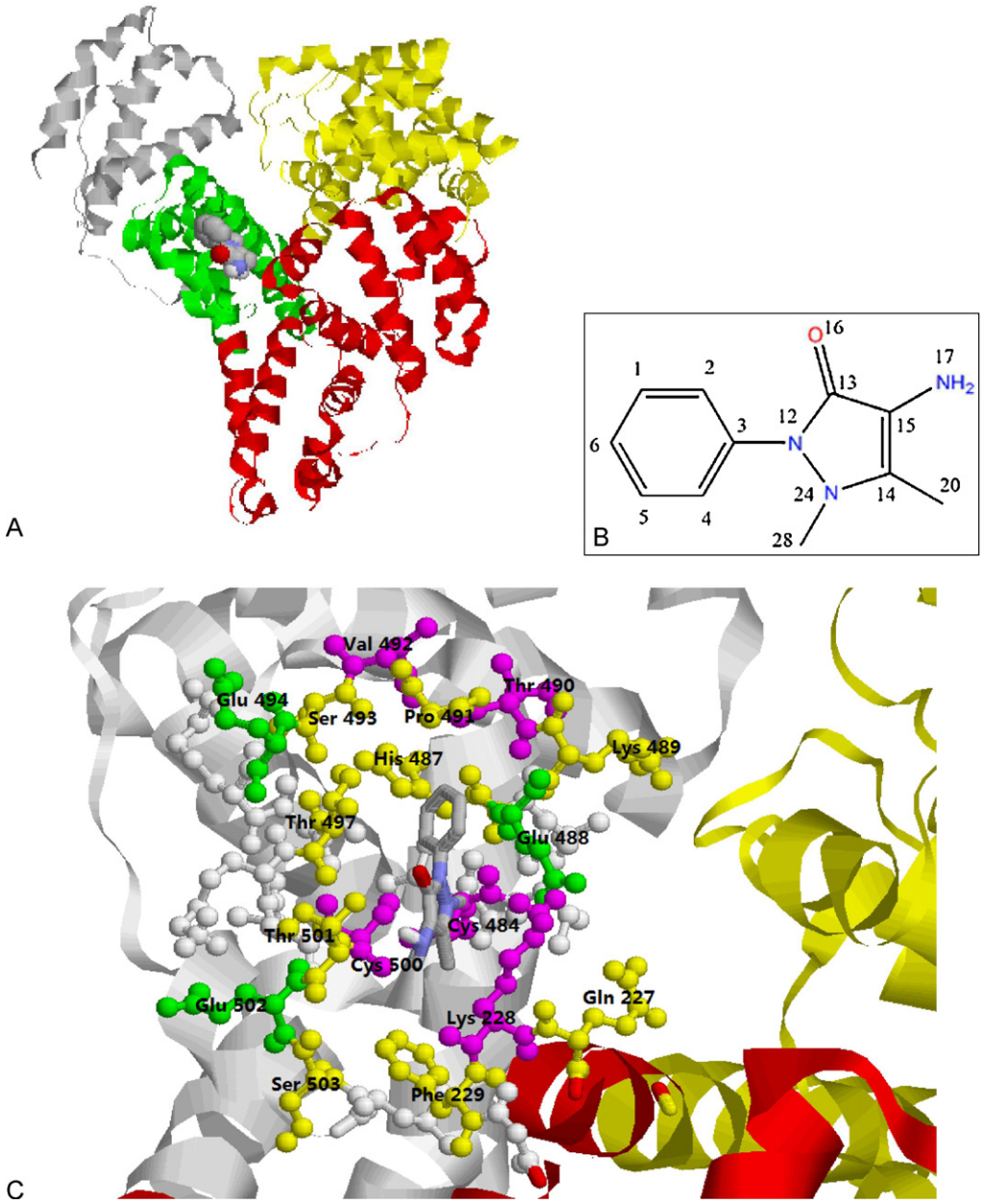

Fig. 4. Docking results of the AAP and BSA system. (A) Binding site of AAP to BSA. AAP is shown in space-filling model. The subdomains of BSA are color-coded as follows: yellow, I; red, II; green, IIIA; white, IIIB. (B) 2D structure of AAP with atom numbers. (C) Detailed illustration of the binding between AAP and BSA. The subdomains of BSA are color-coded as follows: yellow, I; red, II; white, III. (For interpretation of the references to color in this figure legend, the reader is referred to the web version of the article.)

scanning of the excitation and emission monochromators while maintaining a constant wavelength interval between them. The shift in the emission maximum (λ_{em}) reflects the changes of polarity around the chromophore molecule [44]. When the wavelength interval ($\Delta\lambda$) between the excitation and emission wavelength is stabilized at 15 or 60 nm, the synchronous fluorescence gives characteristic information of tyrosine residues or tryptophan residues, respectively [45]. The synchronous fluorescence spectra at these two different wavelength intervals are presented in Fig. 5.

As the concentration of AAP increased gradually, the synchronous fluorescence intensity decreased and an obvious red shift of the tyrosine peak can be observed in Fig. 5A, which indicated that the hydrophobicity of the tyrosine residues decreased and the tyrosines buried in the nonpolar hydrophobic cavities were moved to a more hydrophilic environment. In Fig. 5B, the emission peaks of tryptophan residues had a very slight red shift, which indicated that AAP had a weaker effect on the microenvironment of tryptophan residues. It is shown in Fig. 6 that the slope was higher when $\Delta\lambda$ was 15 nm indicating AAP was closer to the tyrosine residues than to the tryptophan residues. In conclusion, because the binding site of AAP was closer to tyrosine residues, the microenvironments of tyrosine residues were influenced more than those of tryptophan residues.

3.6.2. *UV–vis absorption spectroscopy*

UV–vis absorption can be applied to explore protein structural changes and to investigate protein-ligand complex formation. The UV–vis absorption spectra of BSA in the presence and absence of AAP are shown in Fig. 7. The absorption peak of BSA at about 208 nm reflects the framework conformation of the protein [46]. As the concentration of AAP increased, the absorbance of BSA decreased and the maximum peak position of AAP–BSA was red-

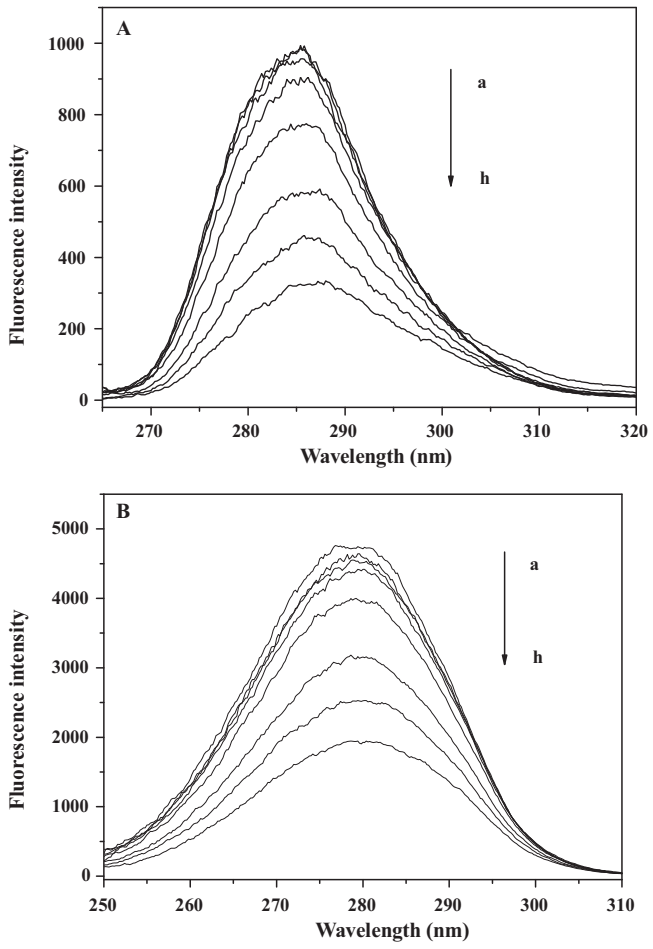

Fig. 5. Synchronous fluorescence spectra of BSA. *Conditions*: (A) $\Delta\lambda = 15$ nm and (B) $\Delta\lambda = 60$ nm. BSA 1.0×10^{-6} mol L^{-1}; AAP (a–h) 0 mol L^{-1}, 1×10^{-6} mol L^{-1}, 5×10^{-6} mol L^{-1}, 1×10^{-5} mol L^{-1}, 2×10^{-5} mol L^{-1}, 4×10^{-5} mol L^{-1}, 6×10^{-5} mol L^{-1}, 8×10^{-5} mol L^{-1}; pH 7.4; $T = 294$ K.

shifted. which indicated that the hydrophobicity decreased and the peptide strands of BSA became more extended [47]. Therefore, the binding between AAP and BSA leads to changes in the BSA conformation.

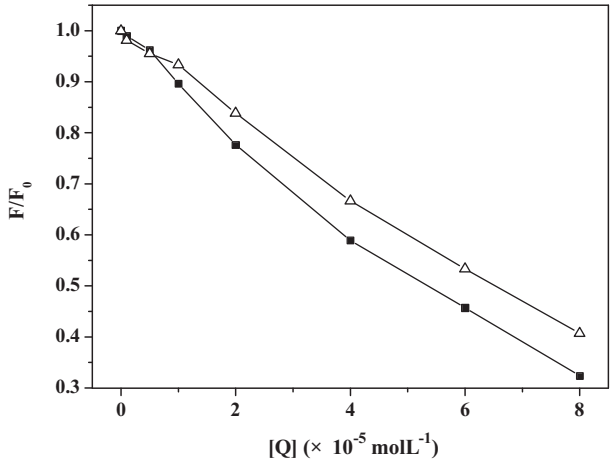

Fig. 6. The quenching of BSA synchronous fluorescence by AAP. *Conditions*: BSA 1.0×10^{-6} mol L^{-1}; (■) $\Delta\lambda = 15$ nm and (△) $\Delta\lambda = 60$ nm.

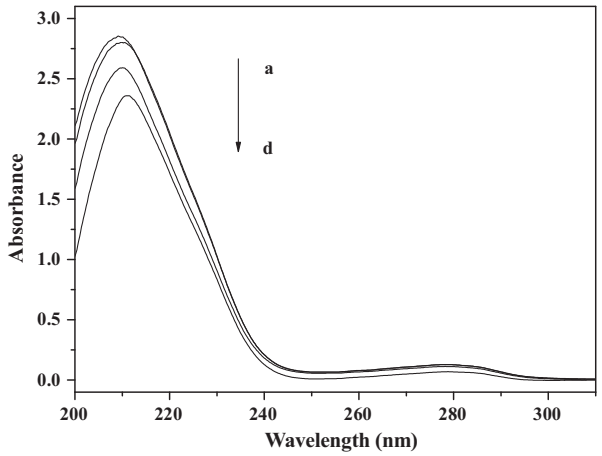

Fig. 7. Absorption spectra of BSA in the presence of different concentrations of AAP. *Conditions*: BSA 2.5×10^{-6} mol L^{-1}; AAP concentrations in AAP–BSA system (a–d) were 0, 1×10^{-5}, 4×10^{-5}, 8×10^{-5} mol L^{-1}. AAP of the same concentration was used as the reference solution.

3.6.3. Circular dichroism spectroscopy

CD is a sensitive technique to monitor the secondary structure of protein. The CD spectra of BSA in the absence and presence of AAP are shown in Fig. 8. The CD spectra of BSA exhibited two negative bonds in the ultraviolet region at 208 and 222 nm, which are characteristic of α-helix of proteins [43]. The α-helical content of BSA can be calculated from Eqs. (6) and (7) [48].

$$\mathrm{MRE} = \frac{\mathrm{ObservedCD\ (mdeg)}}{C_P n l \times 10} \tag{6}$$

where C_P is the molar concentration of the protein, n is the number of amino acid residues and l is the path length.

$$\alpha\text{-Helix}\,(\%) = \frac{-\mathrm{MRE}_{208} - 4000}{33,000 - 4000} \times 100 \tag{7}$$

where MRE_{208} is the observed MRE (mean residual ellipticity) at 208 nm, 4000 is the MRE of the β-form and random coil conformation cross at 208 nm, and 33,000 is the MRE value of a pure α-helix at 208 nm. From the above equations, quantitative results for the amount of α-helix in the secondary structure of BSA were obtained. With the addition of AAP to BSA (20:1 and 50:1), the α-helical content decreased from 69.3% in free BSA to 65.1% and 63.5%, respectively. The decreased percentage of α-helix indicated that AAP bound to the amino acid residues of the backbone chain of

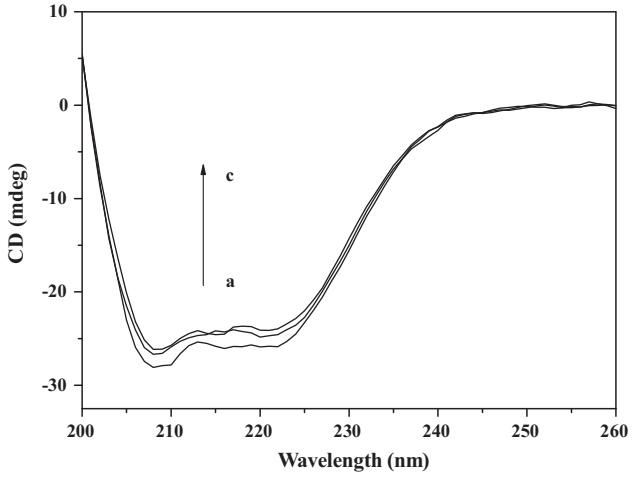

Fig. 8. CD spectra of the BSA and AAP–BSA system. *Conditions*: BSA 2×10^{-7} mol L^{-1}; AAP concentrations in the AAP–BSA system (a–c) were 0, 4×10^{-6}, 1×10^{-5} mol L^{-1}.

BSA, destroyed the hydrogen bonding networks and caused partial unfolding of the protein [49]. It can be concluded that the binding of AAP to BSA induces conformational changes in BSA, which is similar with the effect of AAP on the conformational changes of bovine hemoglobin.

4. Conclusions

In this study, the interaction of AAP with BSA was investigated by multiple spectroscopic techniques and molecular docking simulation. AAP effectively quenched the fluorescence of BSA by a static quenching process. Based on the results of binding capacity and calculated thermodynamic parameters, we concluded that the positively charged AAP can spontaneously bind with the negatively charged BSA through electrostatic forces. Both the molecular docking study and site-competitive replacement experiments showed that AAP bound to BSA on the subdomain IIIA and the exact conformation of AAP in binding site was also explored. The synchronous fluorescence, UV–vis absorption and CD spectra revealed that the microenvironment and conformation of BSA were demonstrably changed in the presence of AAP. The skeletal structure of BSA loosened, exposing internal hydrophobic aromatic ring amino acids and peptide strands to the solution. All these experimental results and theoretical data demonstrate that AAP has an obvious denaturing effect on BSA.

Acknowledgments

The work is supported by NSFC (20875055), the Cultivation Fund of the Key Scientific and Technical Innovation Project, Ministry of Education of China (708058), and Key Science-Technology Project in Shandong Province (2008GG10006012) are also acknowledged. The authors thank Dr. Pamela Holt for assistance in editing the manuscript.

References

[1] D.C. Carter, J.X. Ho, Structure of serum albumin, Adv. Protein Chem. 45 (1994) 153–176.
[2] A. Varshney, P. Sen, E. Ahmad, M. Rehan, N. Subbarao, R.H. Khan, Ligand binding strategies of human serum albumin: how can the cargo be utilized? Chirality 22 (2010) 77–87.
[3] A. Papadopoulou, R.J. Green, R.A. Frazier, Interaction of flavonoids with bovine serum albumin: a fluorescence quenching study, J. Agric. Food Chem. 53 (2005) 158–163.
[4] S. Neelam, M. Gokara, B. Sudhamalla, D.G. Amooru, R. Subramanyam, Interaction studies of coumaroyltyramine with human serum albumin and its biological importance, J. Phys. Chem. B 114 (2010) 3005–3012.
[5] M. Gulden, S. Morchel, S. Tahan, H. Seibert, Impact of protein binding on the availability and cytotoxic potency of organochlorine pesticides and chlorophenols in vitro, Toxicology 175 (2002) 201–213.
[6] Z. Chi, R. Liu, Y. Teng, X. Fang, C. Gao, Binding of oxytetracycline to bovine serum albumin: spectroscopic and molecular modeling investigations, J. Agric. Food Chem. 58 (2010) 10262–10269.
[7] N.J. Turro, X.-G. Lei, Spectroscopic probe analysis of protein-surfactant interactions: the BSA/SDS system, Langmuir 11 (1995) 2525–2533.
[8] J. Tian, J. Liu, Z. Hu, X. Chen, Interaction of Wogonin with bovine serum albumin, Bioorg. Med. Chem. 13 (2005) 4124–4129.
[9] R. Liu, F. Sun, L. Zhang, W. Zong, X. Zhao, L. Wang, R. Wu, X. Hao, Evaluation on the toxicity of nanoAg to bovine serum albumin, Sci. Total Environ. 407 (2009) 4184–4188.
[10] M.N. Jones, Surfactant interactions with biomembranes and proteins, Chem. Soc. Rev. 21 (1992) 127–136.
[11] N. Wang, L. Ye, F. Yan, R. Xu, Spectroscopic studies on the interaction of azelnidipine with bovine serum albumin, Int. J. Pharm. 351 (2008) 55–60.
[12] L.A. MacManus-Spencer, M.L. Tse, P.C. Hebert, H.N. Bischel, R.G. Luthy, Binding of perfluorocarboxylates to serum albumin: a comparison of analytical methods, Anal. Chem. 82 (2010) 974–981.
[13] Y.M. Chen, Y.P. Chen, Measurements for the solid solubilities of antipyrine, 4-aminoantipyrine and 4-dimethylaminoantipyrine in supercritical carbon dioxide, Fluid Phase Equilib. 282 (2009) 82–87.
[14] A. Lang, C. Hatscher, C. Wiegert, P. Kuhl, Protease-catalysed coupling of N-protected amino acids and peptides with 4-aminoantipyrine, Amino Acids 36 (2009) 333–340.
[15] S. Cunha, S.M. Oliveira, M.T. Rodrigues, R.M. Bastos, J. Ferrari, C.M.A. de Oliveira, L. Kato, H.B. Napolitano, I. Vencato, C. Lariucci, Structural studies of 4-aminoantipyrine derivatives, J. Mol. Struct. 752 (2005) 32–39.
[16] S. Prasad, R.K. Agarwal, Cobalt(II) complexes of various thiosemicarbazones of 4-aminoantipyrine: syntheses, spectral, thermal and antimicrobial studies, Transit. Met. Chem. 32 (2007) 143–149.
[17] J.F. Van Staden, N.W. Beyene, R.I. Stefan, H.Y. Aboul-Enein, Sequential injection spectrophotometric determination of ritodrine hydrochloride using 4-aminoantipyrine, Talanta 68 (2005) 401–405.
[18] J. Kasthuri, J. Santhanalakshmi, N. Rajendiran, Platinum nanoparticle catalysed coupling of phenol derivatives with 4-aminoantipyrine in aqueous medium, Transit. Met. Chem. 33 (2008) 899–905.
[19] C.Z. Katsaounos, E.K. Paleologos, D.L. Giokas, M.I. Karayannis, The 4-aminoantipyrine method revisited: determination of trace phenols by micellar assisted preconcentration, Int. J. Environ. Anal. Chem. 83 (2003) 507–514.
[20] A.M. Vinagre, E.F. Collares, Effect of 4-aminoantipyrine on gastric compliance and liquid emptying in rats, Braz. J. Med. Biol. Res. 40 (2007) 903–909.
[21] S.G. Sunderji, A. El Badry, E.R. Poore, J.P. Figueroa, P.W. Nathanielsz, The effect of myometrial contractures on uterine blood flow in the pregnant sheep at 114 to 140 days' gestation measured by the 4-aminoantipyrine equilibrium diffusion technique, Am. J. Obstet. Gynecol. 149 (1984) 408–412.
[22] A. El Badry, J.P. Figueroa, E.R. Poore, S. Sunderji, S. Levine, M.D. Mitchell, P.W. Nathanielsz, Effect of fetal intravascular 4-aminoantipyrine infusions on myometrial activity (contractures) at 125 to 143 days' gestation in the pregnant sheep, Am. J. Obstet. Gynecol. 150 (1984) 474–479.
[23] S.C. Pierre, R. Schmidt, C. Brenneis, M. Michaelis, G. Geisslinger, K. Scholich, Inhibition of cyclooxygenases by dipyrone, Br. J. Pharmacol. 151 (2007) 494–503.
[24] Y. Teng, R. Liu, S. Yan, X. Pan, P. Zhang, M. Wang, Spectroscopic investigation on the toxicological interactions of 4-aminoantipyrine with bovine hemoglobin, J. Fluoresc. 20 (2010) 381–387.
[25] H.M. Berman, J. Westbrook, Z. Feng, G. Gilliland, T.N. Bhat, H. Weissig, I.N. Shindyalov, P.E. Bourne, The Protein Data Bank, Nucleic Acids Res. 28 (2000) 235–242.
[26] R. Karchin, M. Cline, K. Karplus, Evaluation of local structure alphabets based on residue burial, Proteins 55 (2004) 508–518.
[27] R. Karchin, M. Cline, Y. Mandel-Gutfreund, K. Karplus, Hidden Markov models that use predicted local structure for fold recognition: alphabets of backbone geometry, Proteins 51 (2003) 504–514.
[28] B.K. Sahoo, K.S. Ghosh, S. Dasgupta, Investigating the binding of curcumin derivatives to bovine serum albumin, Biophys. Chem. 132 (2008) 81–88.
[29] S.S. Sur, L.D. Rabbani, L. Libman, E. Breslow, Fluorescence studies of native and modified neurophysins. Effects of peptides and pH, Biochemistry 18 (1979) 1026–1036.
[30] J.S. Mandeville, H.A. Tajmir-Riahi, Complexes of dendrimers with bovine serum albumin, Biomacromolecules 11 (2010) 465–472.
[31] Y.Z. Zhang, B. Zhou, X.P. Zhang, P. Huang, C.H. Li, Y. Liu, Interaction of malachite green with bovine serum albumin: determination of the binding mechanism and binding site by spectroscopic methods, J. Hazard. Mater. 163 (2009) 1345–1352.
[32] S. Soares, N. Mateus, V. Freitas, Interaction of different polyphenols with bovine serum albumin (BSA) and human salivary alpha-amylase (HSA) by fluorescence quenching, J. Agric. Food Chem. 55 (2007) 6726–6735.
[33] J.R. Lakowicz, G. Weber, Quenching of fluorescence by oxygen. A probe for structural fluctuations in macromolecules, Biochemistry 12 (1973) 4161–4170.
[34] Z.X. Chi, R.T. Liu, B.J. Yang, H. Zhang, Toxic interaction mechanism between oxytetracycline and bovine hemoglobin, J. Hazard. Mater. 180 (2010) 741–747.
[35] X.H. Liu, P.X. Xi, F.J. Chen, Z.H. Xu, Z.Z. Zeng, Spectroscopic studies on binding of 1-phenyl-3-(coumarin-6-yl)sulfonylurea to bovine serum albumin, J. Photochem. Photobiol. B 92 (2008) 98–102.
[36] G. Paramaguru, A. Kathiravan, S. Selvaraj, P. Venuvanalingam, R. Renganathan, Interaction of anthraquinone dyes with lysozyme: evidences from spectroscopic and docking studies, J. Hazard. Mater. 175 (2010) 985–991.
[37] P.D. Ross, S. Subramanian, Thermodynamics of protein association reactions: forces contributing to stability, Biochemistry 20 (1981) 3096–3102.
[38] S.N. Khan, B. Islam, R. Yennamalli, A. Sultan, N. Subbarao, A.U. Khan, Interaction of mitoxantrone with human serum albumin: spectroscopic and molecular modeling studies, Eur. J. Pharm. Sci. 35 (2008) 371–382.
[39] X.Y. Hu, J.A. Yang, C.Z. Yang, J.D. Zhang, UV/H_2O_2 degradation of 4-aminoantipyrine: a voltammetric study, Chem. Eng. J. 161 (2010) 68–72.
[40] B.K. Paul, A. Samanta, N. Guchhait, Exploring hydrophobic subdomain IIA of the protein bovine serum albumin in the native, intermediate, unfolded, and refolded states by a small fluorescence molecular reporter, J. Phys. Chem. B 114 (2010) 6183–6196.
[41] N. Zhou, Y.Z. Liang, P. Wang, 18beta-Glycyrrhetinic acid interaction with bovine serum albumin, J. Photochem. Photobiol. A 185 (2007) 271–276.

[42] H. Bian, M. Li, Q. Yu, Z. Chen, J. Tian, H. Liang, Study of the interaction of artemisinin with bovine serum albumin, Int. J. Biol. Macromol. 39 (2006) 291–297.
[43] J.Q. Lu, F. Jin, T.Q. Sun, X.W. Zhou, Multi-spectroscopic study on interaction of bovine serum albumin with lomefloxacin-copper(II) complex, Int. J. Biol. Macromol. 40 (2007) 299–304.
[44] Y.Q. Wang, H.M. Zhang, G.C. Zhang, S.X. Liu, Q.H. Zhou, Z.H. Fei, Z.T. Liu, Studies of the interaction between paraquat and bovine hemoglobin, Int. J. Biol. Macromol. 41 (2007) 243–250.
[45] M. Guo, W.J. Lu, M.H. Li, W. Wang, Study on the binding interaction between carnitine optical isomer and bovine serum albumin, Eur. J. Med. Chem. 43 (2008) 2140–2148.
[46] Q. Yang, J. Liang, H. Han, Probing the interaction of magnetic iron oxide nanoparticles with bovine serum albumin by spectroscopic techniques, J. Phys. Chem. B 113 (2009) 10454–10458.
[47] Y.J. Hu, Y. Liu, H.B. Wang, X.H. Xiao, S.S. Qu, Study of the interaction between monoammonium glycyrrhizinate and bovine serum albumin, J. Pharm. Biomed. Anal. 36 (2004) 915–919.
[48] H.R. De Jonge, Toxicity of tetracyclines in rat-small-intestinal epithelium and liver, Biochem. Pharmacol. 22 (1973) 2659–2677.
[49] S.M.T. Shaikh, J. Seetharamappa, P.B. Kandagal, D.H. Manjunatha, S. Ashoka, Spectroscopic investigations on the mechanism of interaction of bioactive dye with bovine serum albumin, Dyes Pigments 74 (2007) 665–671.